

## Unified Description of Electron-Nucleus Scattering within the Spectral Function Formalism

Noemi Rocco,<sup>1</sup> Alessandro Lovato,<sup>2</sup> and Omar Benhar<sup>1,3</sup>

<sup>1</sup>*INFN and Department of Physics, "Sapienza" University, I-00185 Roma, Italy*

<sup>2</sup>*Physics Division, Argonne National Laboratory, Argonne, Illinois 60439, USA*

<sup>3</sup>*Center for Neutrino Physics, Virginia Tech, Blacksburg, Virginia 24061, USA*

(Received 23 December 2015; published 11 May 2016)

The formalism based on factorization and nuclear spectral functions has been generalized to treat transition matrix elements involving two-nucleon currents, whose contribution to the nuclear electromagnetic response in the transverse channel is known to be significant. We report the results of calculations of the inclusive electron-carbon cross section, showing that the inclusion of processes involving two-nucleon currents appreciably improves the agreement between theory and data in the dip region, between the quasielastic and  $\Delta$ -production peaks. The relation to approaches based on the independent particle of the nucleus and the implications for the analysis of flux-integrated neutrino-nucleus cross sections are discussed.

DOI: 10.1103/PhysRevLett.116.192501

The nuclear response to electromagnetic interactions is determined by a variety of mechanisms—reflecting both nuclear and nucleon excitation modes—whose contributions strongly depend on the energy and momentum transfer,  $\omega$  and  $\mathbf{q}$ .

In the kinematical region corresponding to  $|\mathbf{q}| \gtrsim \pi/d$ , with  $d$  being the average nucleon-nucleon ( $NN$ ) distance, interactions predominantly involve individual nucleons and, depending on energy transfer, may give rise to different hadronic final states. At  $\omega \approx Q^2/2m$ , where  $Q^2 = \mathbf{q}^2 - \omega^2$  and  $m$  is the nucleon mass, the dominant mechanism is quasielastic scattering, in which the nucleon is left in its ground state and no  $\pi$  mesons are produced. With increasing  $\omega$ , the composite nature of the nucleon shows up through the excitation of resonances—the most prominent of which is the  $\Delta$ , with mass  $m_\Delta = 1232$  MeV—and breakup of the nucleon itself, followed by hadronization of the debris. The corresponding final states are characterized by the presence of one or more  $\pi$  mesons, respectively.

Reaction mechanisms involving two target constituents—for example, the process in which the virtual photon couples to a meson exchanged between interacting nucleons—also play an important role in determining the nuclear response in the transverse channel. They have long been shown to provide a significant amount of strength in the dip region, between the quasielastic and  $\Delta$ -production peaks [1].

The occurrence of two-nucleon components in the nuclear electromagnetic current is dictated by current conservation and isospin dependence of nuclear interactions [2]. Therefore, a coherent treatment of one- and two-nucleon current contributions, including the effects of interference between the corresponding transition matrix elements, is needed to achieve a complete description of the observed electron-nucleus cross sections.

The *ab initio* approach based on nuclear many-body theory and realistic nuclear Hamiltonians—strongly constrained by the properties of two- and three-nucleon systems—provides a fully consistent framework for the calculation of the nuclear electromagnetic responses in the regime of low to moderate momentum transfer, typically  $|\mathbf{q}| \lesssim 500$  MeV, in which the nuclear initial and final states can be described within the nonrelativistic approximation, and the nonrelativistic reduction of the currents is expected to be applicable [3–7].

At high momentum transfer, however, neither the nuclear final state nor the current can be treated using the nonrelativistic formalism, because the former involves at least one nucleon carrying large momentum,  $\sim \mathbf{q}$ , while the latter explicitly depends on  $\mathbf{q}$ . To circumvent this difficulty, theoretical calculations of the two-nucleon current contributions to the nuclear cross section have been carried out within somewhat oversimplified models, in which relativistic effects are taken into account at the expense of a realistic description of nuclear structure and dynamics [8–11].

The formalism based on factorization of the nuclear transition matrix elements [12–14] allows us to combine a fully relativistic description of the electromagnetic interaction with an accurate treatment of nuclear dynamics, in which the effect of  $NN$  correlations is properly taken into account. This scheme, providing a remarkably accurate description of the available data in the kinematical region in which quasielastic single-nucleon knockout is the dominant reaction mechanism [15], has been recently generalized to include the contributions of the two-nucleon currents [16].

The analysis of Ref. [16] was restricted to the electromagnetic response of carbon in the transverse channel at fixed momentum transfer  $|\mathbf{q}| = 570$  MeV, and neglected

final state interactions (FSI) between the struck nucleon and the spectator particles. In this Letter, we report the results of calculations of the *inclusive* electron-carbon cross section at  $300 \lesssim |\mathbf{q}| \lesssim 800$  MeV, carried out taking into account both the elastic and inelastic channels, two-nucleon currents, and FSI effect. We emphasize that in our work the relativistic treatment of the two-nucleon currents is associated, for the first time, with a description of the dynamics that goes beyond the independent particle model of the nucleus.

In interacting many-body systems, processes involving one- and two-nucleon currents are inextricably related, as they both lead to the appearance of two-particle–two-hole ( $2p2h$ ) final states. As a consequence, the corresponding transition amplitudes interfere, and must be treated in a consistent fashion [5].

Neglecting the contribution of final states involving more than two nucleons in the continuum, the cross section can be written as

$$d\sigma \propto L_{\mu\nu} W^{\mu\nu} = L_{\mu\nu} (W_{1p1h}^{\mu\nu} + W_{2p2h}^{\mu\nu}), \quad (1)$$

where the label  $nph$  refers to  $n$ -particle– $n$ -hole final states and the tensor  $L_{\mu\nu}$  is completely determined by lepton kinematics. The target response tensor  $W^{\mu\nu}$ , on the other hand, is written in terms of matrix elements of the nuclear current operator between the target ground state and the hadronic final states.

The current entering the definition of the  $2p2h$  component  $W_{2p2h}^{\mu\nu}$  can be cast in the form

$$J^\mu(\mathbf{k}_1, \mathbf{k}_2) = j_1^\mu(\mathbf{k}_1)\delta(\mathbf{k}_2) + j_2^\mu(\mathbf{k}_2)\delta(\mathbf{k}_1) + j_{12}^\mu(\mathbf{k}_1, \mathbf{k}_2), \quad (2)$$

clearly showing how the total momentum transfer,  $\mathbf{q} = \mathbf{k}_1 + \mathbf{k}_2$ , is shared between the two nucleons involved in the electromagnetic interaction, labeled by the indices 1 and 2.

The Feynman diagrams of Fig. 1, in which  $\mathbf{h}, \mathbf{h}'$  and  $\mathbf{p}, \mathbf{p}'$  label the momenta of the hole and particle states, respectively, illustrate the different contributions to  $j_{12}^\mu(\mathbf{k}_1, \mathbf{k}_2)$ . In this work we have considered two-body currents of two types. The one associated with the exchange of a  $\pi$  meson is required by current conservation. Hence, its expression is determined—at least in principle—by the structure of the  $NN$  potential.

Figure 1(b), featuring a  $\gamma\pi\pi$  vertex, is associated with the “pion-in-flight” term, while the sum of Fig. 1(a), involving a  $\gamma\pi NN$  vertex, and the one obtained interchanging particles 1 and 2 accounts for the “seagull,” or “contact” contribution. Figures 1(c) and 1(d), as well as the corresponding two in which particles 1 and 2 are interchanged, are associated with two-body current terms involving a  $\Delta$  resonance in the intermediate state. Owing to the purely transverse nature of this current, their form is not subject to

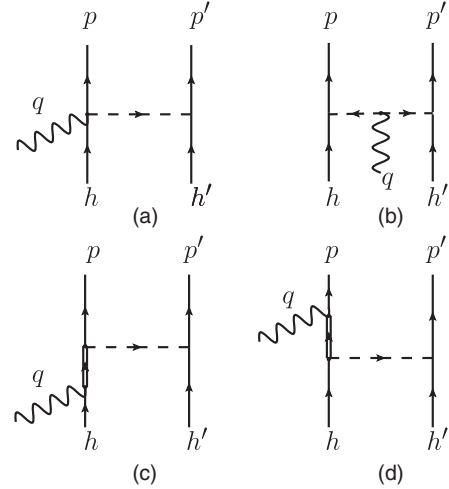


FIG. 1. Free-space meson exchange current diagrams. The first two correspond to  $\pi$ -meson exchange: diagram (a) and the one obtained interchanging particle 1 and 2 represent the contact or seagull contribution, while diagram (b) is the pion-in-flight term. Diagrams (c) and (d), and the additional two resulting from the interchange  $1 \leftrightarrow 2$ , involve a  $\Delta$ -resonance excitation.

current-conservation constraints, and is therefore largely model dependent [2]. In order to make contact between our results and those obtained by Dekker *et al.* [9] and De Pace *et al.* [11], we have used the fully relativistic expression of the two-body currents reported in their papers, with the same form factors and  $\Delta$  width.

The factorization ansatz amounts to writing the matrix elements describing transitions from the ground state to  $2p2h$  final states in terms of nuclear amplitudes and matrix elements of the one- and two-body current operators between free-nucleon states. For the one-nucleon current, one finds [14,16]

$$\langle 0 | j_1^\mu | \mathbf{h} \mathbf{h}' \mathbf{p} \mathbf{p}' \rangle = \int d^3 k \Phi_k^{hh'p'} \langle \mathbf{k} | j_1^\mu | \mathbf{p} \rangle, \quad (3)$$

where the state  $|\mathbf{k}\rangle$  describes a free nucleon carrying momentum  $\mathbf{k}$ , while the overlap between the target ground state and the  $2h1p$  state of the residual  $(A-1)$ -particle system, in which one nucleon is excited to the continuum, is written in the form

$$\Phi_k^{hh'p'} = \langle 0 | \{ |\mathbf{k}\rangle \otimes | \mathbf{h} \mathbf{h}' \mathbf{p}' \rangle \}. \quad (4)$$

Application of the same scheme to the matrix element of the two-nucleon current operator leads to the expression [16]

$$\langle 0 | j_{12}^\mu | \mathbf{h} \mathbf{h}' \mathbf{p} \mathbf{p}' \rangle = \int d^3 k d^3 k' \Phi_{kk'}^{hh'p'} \langle \mathbf{k} \mathbf{k}' | j_{12}^\mu | \mathbf{p} \mathbf{p}' \rangle, \quad (5)$$

with the nuclear amplitude, involving  $2h$  bound states of the  $(A-2)$ -nucleon spectator system, given by

$$\Phi_{kk'}^{hh'} = \langle 0 | \{ | \mathbf{k} \mathbf{k}' \rangle \otimes | \mathbf{h} \mathbf{h}' \rangle \}. \quad (6)$$

Using the above results, the  $2p2h$  contribution to the nuclear response tensor can be decomposed according to

$$W_{2p2h}^{\mu\nu} = W_{2p2h,11}^{\mu\nu} + W_{2p2h,22}^{\mu\nu} + W_{2p2h,12}^{\mu\nu}. \quad (7)$$

The first term comprises the squared amplitudes involving only the one-nucleon current. Note that the occurrence of these matrix elements is a genuine correlation effect, not accounted for within the independent particle model. As a consequence, the calculation of  $W_{2p2h,11}^{\mu\nu}$ , describing processes in which the momentum  $\mathbf{q}$  is transferred to a single high-momentum nucleon, requires the continuum component of the hole spectral function [17,18].

The second term on the right-hand side of Eq. (7), involving the matrix elements of the two-nucleon current, is written in terms of the two-nucleon spectral function [19]. The explicit expressions of  $W_{2p2h,11}^{\mu\nu}$  and  $W_{2p2h,22}^{\mu\nu}$  are reported in Ref. [16].

Finally,  $W_{2p2h,12}^{\mu\nu}$ , taking into account interference contributions, involves the nuclear overlaps defined in both Eqs. (4) and (6). The resulting expression is

$$\begin{aligned} W_{2p2h,12}^{\mu\nu} = & \int d^3k d^3\xi d^3\xi' d^3hd^3h'd^3pd^3p' \Phi_{\xi\xi'}^{hh'*} \\ & \times [\Phi_k^{hh'p'} \langle \mathbf{k} | j_1^\mu | \mathbf{p} \rangle + \Phi_k^{hh'p} \langle \mathbf{k} | j_2^\mu | \mathbf{p}' \rangle] \\ & \times \langle \mathbf{p} \mathbf{p}' | j_{12}^\nu | \xi, \xi' \rangle \delta(\mathbf{h} + \mathbf{h}' + \mathbf{q} - \mathbf{p} - \mathbf{p}') \\ & \times \delta(\omega + e_h + e_{h'} - e_p - e_{p'}) \theta(|\mathbf{p}| - k_F) \\ & \times \theta(|\mathbf{p}'| - k_F) + \text{H.c.} \end{aligned} \quad (8)$$

We have compared the results of our approach to the measured electron-carbon cross sections in two different kinematical setups, corresponding to momentum transfer  $300 \lesssim |\mathbf{q}| \lesssim 800$  MeV. The calculations have been carried out following Ref. [16], using the carbon spectral function of Ref. [20] and the  $1h$  contribution to the spectral function of isospin-symmetric nuclear matter of Ref. [17]. The  $2h1p$  amplitude, needed to evaluate the interference term, has also been computed for nuclear matter at equilibrium density. In the quasielastic channel we have adopted the parametrization of the nucleon form factors of Ref. [21], whereas the inelastic nucleon structure functions have been taken from Refs. [22,23].

Figure 2 shows the electron-carbon cross section at beam energy  $E_e = 680$  MeV and scattering angle  $\theta_e = 36$  deg [Fig. 2(a)] and  $E_e = 1300$  MeV and  $\theta_e = 37.5$  deg [Fig. 2(b)]. The solid and dashed lines correspond to the results of the full calculation and to the one-body current contribution, respectively. The pure two-body current contribution and the one arising from interference are illustrated by the dot-dashed and dotted lines. In the kinematics of Fig. 2(a) the two-body currents play an

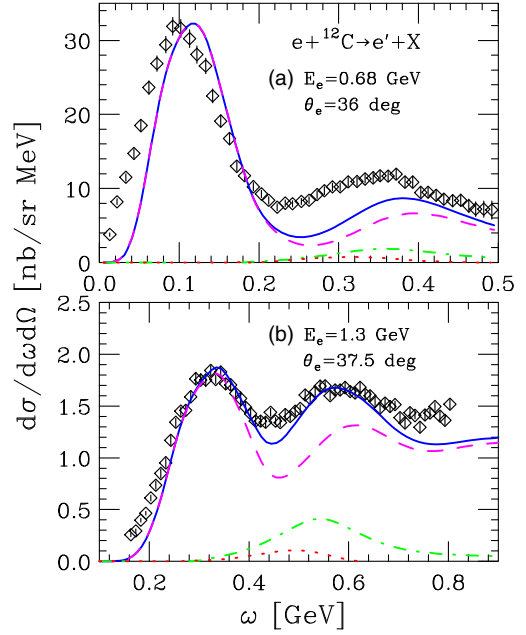


FIG. 2. (a) Double differential cross section of the process  $e + {}^{12}\text{C} \rightarrow e' + X$  at beam energy  $E_e = 680$  MeV and scattering angle  $\theta_e = 37.5$  deg. The solid line shows the result of the full calculation, while the dashed line has been obtained including the one-body current only. The contributions arising from two-nucleon currents are illustrated by the dot-dashed and dotted lines, corresponding to the pure two-body current transition probability and to the interference term, respectively. The experimental data are taken from Ref. [24]. (b) Same as (a) but for  $E_e = 1300$  MeV and  $\theta_e = 37.5$  deg. The experimental data are taken from Ref. [25].

almost negligible role. The significant lack of strength in the  $\Delta$ -production region, discussed in Ref. [26], is likely to be due to the inadequacy of the structure functions of Refs. [22,23] to describe the region of  $Q^2 \lesssim 0.2$  GeV<sup>2</sup>, while the shift in the position of the quasielastic peak has to be ascribed to the effects of FSI, which are not taken into account.

At the larger beam energy and  $Q^2$  corresponding to Fig. 2(b), the agreement between theory and data is significantly improved, and the contribution of the two-nucleon currents turns out to substantially increase the cross section in the dip region and beyond.

In inclusive processes, FSI have two effects: a shift of the cross section, arising from the interaction between the struck nucleon and the mean field generated by the spectator particles, and a redistribution of the strength from the quasielastic peak to the tails. The theoretical approach for the description of FSI within the spectral function formalism is discussed in Refs. [12,13,15,27].

According to Refs. [15,27], the differential cross section can be written in the convolution form

$$d\sigma_{\text{FSI}}(\omega) = \int d\omega' f_{\mathbf{q}}(\omega - \omega' - U_V) d\sigma(\omega'), \quad (9)$$

where  $d\sigma$  denotes the cross section in the absence of FSI, the effects of which are accounted for by the folding function

$$f_q(\omega) = \sqrt{T_A}\delta(\omega) + (1 - \sqrt{T_A})F_q(\omega). \quad (10)$$

The above equations show that inclusion of FSI involves three elements: (i) the real part of the optical potential  $U_V$  extracted from proton-carbon scattering data [28], responsible for the shift in  $\omega$ , (ii) the nuclear transparency  $T_A$  measured in coincidence ( $e, e'p$ ) reactions [29], and (iii) a function  $F_q(\omega)$ , sharply peaked at  $\omega = 0$ , whose width is dictated by the in-medium  $NN$  scattering cross section [27].

A comprehensive analysis of FSI effects on the electron-carbon cross sections has been recently carried out by the authors of Ref. [15]. In this work we have followed closely their approach, using the same input.

Figure 3 illustrates the effects of FSI on the electron-carbon cross section in the kinematical setups of Fig. 2. In Fig. 3(a), both the pronounced shift of the quasielastic peak and the redistribution of the strength are clearly visible, and significantly improve the agreement between theory and data. For larger values of  $Q^2$ , however, FSI play a less relevant, in fact almost negligible, role. This feature is illustrated in Fig. 3(b), showing that at beam energy  $E_e = 1.3$  GeV and scattering angle  $\theta_e = 37.5$  deg, corresponding to  $Q^2 \sim 0.5$  GeV<sup>2</sup>, the results of calculations carried out

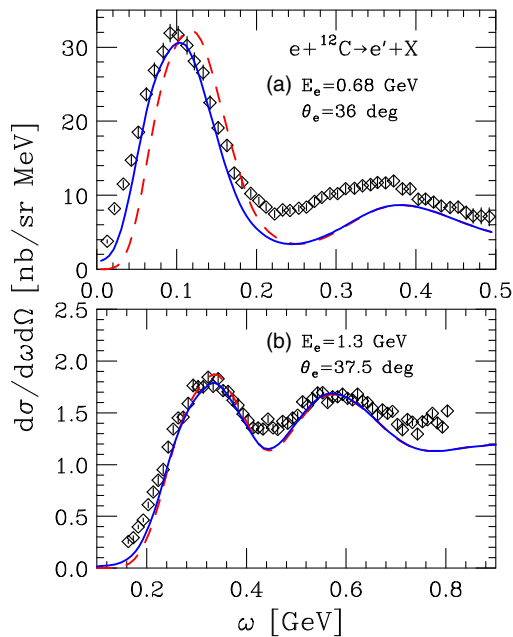


FIG. 3. (a) Double differential electron-carbon cross section at beam energy  $E_e = 680$  MeV and scattering angle  $\theta_e = 36$  deg. The dashed line corresponds to the result obtained neglecting FSI, while the solid line has been obtained within the approach of Ref. [15]. The experimental data are taken from Ref. [24]. (b) Same as (a) but for  $E_e = 1300$  MeV and  $\theta_e = 37.5$  deg. The experimental data are taken from Ref. [25].

with and without inclusion of FSI give very similar results, yielding a good description of the data.

Note that, being transverse in nature, the calculated two-nucleon current contributions to the cross sections exhibit a strong angular dependence. At  $E_e = 1.3$  GeV, we find that the ratio between the integrated strengths in the  $1p1h$  and  $2p2h$  sectors grows from 4% at electron scattering angle  $\theta_e = 10$  deg to 46% at  $\theta_e = 60$  deg.

The results of our work show that the approach based on the generalized factorization ansatz and the spectral function formalism provides a consistent framework for a unified description of the electron-nucleus cross section, applicable in the kinematical regime in which relativistic effects are known to be important.

The extension of our approach to neutrino-nucleus scattering, which does not involve further conceptual difficulties, may offer new insight into the interpretation of the cross section measured by the MiniBooNE Collaboration in the quasielastic channel [30,31]. The excess strength in the region of the quasielastic peak is in fact believed to originate from processes involving two-nucleon currents [32–34], whose contributions are observed at lower muon kinetic energy as a result of the average over the neutrino flux [35]. The strong angular dependence of the two-nucleon current contribution may also provide a clue for the understanding of the differences between the quasielastic cross sections reported by the MiniBooNE Collaboration and the NOMAD Collaboration [36], which collected data using neutrino fluxes with very different mean energies: 880 MeV and 25 GeV, respectively [35].

As a final remark, it has to be pointed out that a clear-cut identification of the variety of reaction mechanisms contributing to the neutrino-nucleus cross section will require a careful analysis of the assumptions underlying different models of nuclear dynamics. All approaches based on the independent particle model fail to properly take into account correlation effects, leading to a significant reduction of the normalization of the shell-model states [37], as well as to the appearance of sizable interference terms in the  $2p2h$  sector. However, in some instances these two deficiencies may largely compensate one another, leading to *accidental* agreement between theory and data. For example, the two-body current contributions computed within our approach turn out to be close to those obtained within the Fermi gas model.

The development of a nuclear model having the predictive power needed for applications to the analysis of future experiments—most notably the Deep Underground Neutrino Experiment (DUNE) [38]—will require that the degeneracy between different approaches be resolved. A systematic comparison between the results of theoretical calculations and the large body of electron scattering data, including both inclusive and exclusive cross sections, will greatly help to achieve this goal.



This research is supported by INFN (Italy) under grant MANYBODY (N. R. and O. B.) and the U.S. Department of Energy, Office of Science, Office of Nuclear Physics, under Contract No. DE-AC02-06CH11357 (A. L.).

- 
- [1] J. W. Van Orden and T. W. Donnelly, *Ann. Phys. (N.Y.)* **131**, 451 (1981).
- [2] D. O. Riska, *Phys. Rep.* **181**, 207 (1989).
- [3] J. E. Amaro, G. Cò, and A. M. Lallena, *Nucl. Phys.* **A578**, 365 (1994).
- [4] J. Carlson and R. Schiavilla, *Rev. Mod. Phys.* **70**, 743 (1998).
- [5] J. Carlson, J. Jourdan, R. Schiavilla, and I. Sick, *Phys. Rev. C* **65**, 024002 (2002).
- [6] A. Lovato, S. Gandolfi, R. Butler, J. Carlson, E. Lusk, S. C. Pieper, and R. Schiavilla, *Phys. Rev. Lett.* **111**, 092501 (2013).
- [7] A. Lovato, S. Gandolfi, J. Carlson, Steven C. Pieper, and R. Schiavilla, *Phys. Rev. C* **91**, 062501(R) (2015).
- [8] W. M. Alberico, M. Ericson, and A. Molinari, *Ann. Phys. (N.Y.)* **154**, 356 (1984).
- [9] M. J. Dekker, P. J. Brussaard, and J. A. Tjon, *Phys. Rev. C* **49**, 2650 (1994).
- [10] A. Gil, J. Nieves, and E. Oset, *Nucl. Phys.* **A627**, 543 (1997).
- [11] A. De Pace, M. Nardi, W. A. Alberico, T. W. Donnelly, and A. Molinari, *Nucl. Phys.* **A726**, 303 (2003).
- [12] O. Benhar, N. Farina, H. Nakamura, M. Sakuda, and R. Seki, *Phys. Rev. D* **72**, 053005 (2005).
- [13] O. Benhar, D. Day, and I. Sick, *Rev. Mod. Phys.* **80**, 189 (2008).
- [14] O. Benhar and N. Rocco, *Adv. High Energy Phys.* **2013**, 912702 (2013).
- [15] A. M. Ankowski, O. Benhar, and M. Sakuda, *Phys. Rev. D* **91**, 033005 (2015).
- [16] O. Benhar, A. Lovato, and N. Rocco, *Phys. Rev. C* **92**, 024602 (2015).
- [17] O. Benhar, A. Fabrocini, and S. Fantoni, *Nucl. Phys.* **A505**, 267 (1989).
- [18] O. Benhar, A. Fabrocini, and S. Fantoni, *Phys. Rev. C* **41**, R24 (1990).
- [19] O. Benhar and A. Fabrocini, *Phys. Rev. C* **62**, 034304 (2000).
- [20] O. Benhar, A. Fabrocini, S. Fantoni, and I. Sick, *Nucl. Phys.* **A579**, 493 (1994).
- [21] R. Bradford, A. Bodek, H. Budd, and J. Arrington, *Nucl. Phys. B, Proc. Suppl.* **159**, 127 (2006).
- [22] A. Bodek and J. L. Ritchie, *Phys. Rev. D* **23**, 1070 (1981).
- [23] A. Bodek *et al.*, *Phys. Rev. D* **20**, 1471 (1979).
- [24] P. Barreau *et al.*, *Nucl. Phys.* **A402**, 415 (1983).
- [25] R. M. Sealock *et al.*, *Phys. Rev. Lett.* **62**, 1350 (1989).
- [26] O. Benhar and D. Meloni, *Phys. Rev. Lett.* **97**, 192301 (2006).
- [27] O. Benhar, *Phys. Rev. C* **87**, 024606 (2013).
- [28] E. D. Cooper, S. Hama, B. C. Clark, and R. L. Mercer, *Phys. Rev. C* **47**, 297 (1993).
- [29] D. Rohe *et al.* (JLAB E97-006 Collaboration), *Phys. Rev. C* **72**, 054602 (2005).
- [30] A. A. Aguilar-Arevalo *et al.* (MiniBooNE Collaboration), *Phys. Rev. D* **81**, 092005 (2010).
- [31] A. A. Aguilar-Arevalo *et al.* (MiniBooNE Collaboration), *Phys. Rev. D* **82**, 092005 (2010).
- [32] M. Martini, M. Ericson, G. Chanfray, and J. Marteau, *Phys. Rev. C* **80**, 065501 (2009); **81**, 045502 (2010).
- [33] J. Nieves, I. R. Simo, and M. J. Vicente Vacas, *Phys. Lett. B* **707**, 72 (2012).
- [34] G. D. Megias *et al.*, *Phys. Rev. D* **91**, 073004 (2015).
- [35] O. Benhar, *J. Phys. Conf. Ser.* **408**, 012042 (2013).
- [36] V. Lyubushkin *et al.* (NOMAD Collaboration), *Eur. Phys. J. C* **63**, 355 (2009).
- [37] O. Benhar, V. R. Pandharipande, and S. C. Pieper, *Rev. Mod. Phys.* **65**, 817 (1993).
- [38] R. Acciarri *et al.* (DUNE Collaboration), arXiv:1512.06148.